scientific reports

Check for updates

OPEN

Delayed, transient, lateralized deficits in pattern separation and pattern completion after focal hippocampal irradiation in humans

Olga A. Krotkova[1]✉, Mikhail V. Galkin[1], Gleb V. Danilov[1], Elena V. Enikolopova[2], Mariya Yu. Kaverina[1], Arina Yu. Kuleva[3], Natalya A. Filchenkova[1], Evgeny M. Amelchenko[4,5], Konstantin V. Anokhin[2], Alexander A. Lazutkin[4,5] & Grigori Enikolopov[4,5]✉

Adult hippocampal neurogenesis is essential for discriminating between similar contexts (pattern separation) in animals. In humans, the link between neurogenesis and pattern separation remains tenuous due to the inherent constraints on manipulating neurogenesis. Here, we report a longitudinal study of patients with benign cavernous sinus meningiomas localized immediately adjacent to the hippocampus. Patients underwent focal stereotactic radiotherapy, which, while targeted at the tumor, inevitably affected the ipsilateral hippocampus. At different timepoints post-therapy (up to 2 years), patients were presented with mnemonic similarity task (MST) to assess pattern separation, pattern completion, and recognition memory. While hippocampal irradiation did not affect the overall recall or recognition memory, we found delayed, transient, laterally-restricted effects on pattern separation and completion. In patients with right-sided (but not left-sided) hippocampal irradiation deficits in pattern separation and completion accumulated by 12 months post-treatment, but returned to the initial levels by 24 months. The observed changes are consistent with the vulnerability of dividing neural progenitors in the dentate gyrus, the protracted maturation of new neurons in the adult human brain, and the involvement of adult-born neurons in pattern separation and pattern completion. Our findings support the notion that ongoing hippocampal neurogenesis contributes to defined cognitive functions in humans.

Keywords Pattern separation, Pattern completion, Hippocampus, Focal irradiation, Adult neurogenesis, Human neurogenesis, Mnemonic similarity task, Laterality, Meningioma

Episodic memory relies, among other processes, on the ability to discriminate between similar but nonidentical contexts presented during the encoding phase (behavioral pattern separation) and to restore a previously learned representation when presented with an incomplete cue during the recall phase (behavioral pattern completion)[1–8]. While conceptually related, pattern separation and pattern completion are not simply complementary and can be experimentally dissociated; moreover, they critically rely on adjacent, but distinct, brain structures, such as the dentate gyrus (DG) and the CA3 region of the hippocampus, respectively[1,8–12].

The DG is distinct from most other brain regions in that it supports the production of new granule neurons from neural stem cells in adulthood[4,13–16]. In rodent models, the generation of new neurons in the DG has been convincingly linked to efficient pattern separation in gain- and loss- of function experiments: suppression of neurogenesis reduces the animals' ability to distinguish between familiar and slightly modified contexts, whereas enhanced neurogenesis improves this ability beyond normal levels[7,17–23].

In humans, the hypothesis that adult hippocampal neurogenesis supports pattern separation is gaining support, primarily from correlational studies involving aging and neurologically impaired populations[1,24–27]. These studies typically use modified versions of MST in which subjects must distinguish a briefly presented visual cue from a new visual cue that carries some, but not full, resemblance to the original cue (pattern

[1]Burdenko National Medical Research Center for Neurosurgery, Moscow, Russian Federation. [2]Lomonosov Moscow State University, Moscow, Russian Federation. [3]Institute of Higher Nervous Activity and Neurophysiology, Moscow, Russian Federation. [4]Center for Developmental Genetics, Stony Brook University, Stony Brook, NY, USA. [5]Department of Anesthesiology, Renaissance Medical School, Stony Brook University, Stony Brook, NY, USA. ✉email: krotkovao@gmail.com; grigori.enikolopov@stonybrook.edu

separation)[1,2,10,24–28]. An overlapping test evaluates the ability to retrieve a memory representation based on partial or degraded cues (pattern completion)[2,10,24,26]. Such tasks reveal that the ability to discriminate between similar contexts decreases with age, stroke, traumatic brain injury, or progression of mild cognitive impairment and Alzheimer's disease—conditions that have been associated with reduced hippocampal neurogenesis in animal models. These findings align with accumulating evidence for lifelong hippocampal neurogenesis in humans, and for its decline in Alzheimer's disease[29–34]. However, a more direct relationship between hippocampal neurogenesis and pattern separation/pattern completion in humans has not been established, largely due to the obvious limitations of intentionally interfering with neurogenesis in human subjects, e.g., by diminishing production of adult-born neurons.

There is a broad range of experimental approaches for eliminating dividing cells and prospective new neurons in animals; this includes genetic techniques[17,18,35], treatment with anti-mitotic factors such as chemotherapeutic agents[18,36,37], and irradiation with X-rays, gamma-rays, or heavy ions[38–47]. Human populations exposed to comparable treatments include cancer patients receiving chemo- or radiotherapy as first-line or adjuvant therapies. However, in most cases, such treatments are either systemic or affect large regions of the brain and are often confounded by the effects of the tumor itself having spread or occupied extended brain areas. As a result, the cognitive and behavioral consequences of such therapies are difficult to reliably ascribe specifically to reduced neurogenesis.

To circumvent these limitations, we focused on a cohort of meningioma patients undergoing focal radiation therapy. Meningiomas are extracerebral, slow-growing, typically benign non-metastatic neoplasms that can be effectively treated with surgery or targeted radiotherapy[48,49]. Specifically, we studied a unique cohort of meningioma patients with the tumors confined to the cavernous sinus, adjacent to the hippocampus. Such patients are successfully treated with stereotactic conformal irradiation[48,49]. While this technique allows for a highly restricted radiation exposure focused on the tumor, in some cases, the beam unavoidably affects adjacent brain structures such as the hippocampus. Because radiation is delivered specifically to eradicate proliferating cells, we posited that in these cases, one of the consequences of therapy might be selective and efficient ablation of the dividing neural stem and progenitor cells of the DG and suppression of the production of new neurons in the DG; this could provide a framework for probing neuropsychological consequences of reduced adult neurogenesis in humans.

We conducted a longitudinal study on this unique patient cohort to investigate the impact of hippocampal irradiation (with presumable disruption of neurogenesis) on human pattern separation and pattern completion abilities, using a modified version of the MST. In particular, considering that a wide range of brain functions exhibits pronounced dependence on the side of the brain[50,51], we modified the tests to assess potential laterality effects with respect to both the location of the tumor and the presentation of the visual stimuli. Our findings reveal a significant reduction in pattern separation and an increase in pattern completion abilities in irradiated patients one year post-irradiation. Importantly, these changes were overcome at the later timepoints. Notably, this protracted time course is comparable with the proposed maturation timeline of adult-born neurons in the human hippocampus[34,52–54]. Remarkably, the deficits were most pronounced in a subcohort of patients with the tumor localized (and thus the radiation treatment conducted) in the vicinity of the right hippocampus, consistent with the reported functional differences between the left and right sides of the brain and of the hippocampus[50,51,55]. Together, our results provide the first evidence of transient reversible changes in pattern separation and pattern completion in humans and suggest that temporary suppression of the hippocampal neurogenesis may underlie these dynamics.

Results

Patient population

We studied meningioma patients with tumors localized to the central part of the skull base, in the cavernous sinus region. Importantly, meningiomas are extracerebral tumors that do not infiltrate the neural tissue, and are typically diagnosed when the tumor begins to exert pressure on adjacent brain structures or involves cranial nerves. While meningiomas most commonly arise on the surface of the frontal and parietal lobes, in the sylvian region, or along the sphenoid ridge, in a small number of cases the growth is limited to the left or right cavernous sinus[48,49]. In the latter case, the tumors are not easily accessible to surgery and are treated by stereotactic irradiation. In a fraction of those cases, the hippocampus is located in the immediate vicinity of the tumor and inevitably falls within the radiation exposure zone.

We selected a group of 28 patients with cavernous sinus meningiomas located in close proximity to the hippocampal region. The group included 24 females and 4 males of median age 52 years, reflecting the known prevalence of meningiomas in females over 50 (Supplementary Table 1). Of these, 15 patients had left-sided localization of the tumor (tumLeft) and 13 had right-sided tumor localization (tumRight). In each case the diagnosis of benign meningioma was made based on the clinical features and the results of MRI. The control group comprised 29 healthy individuals matched for age, gender, and education.

Treatment

The current standard of treatment of skull base meningiomas is stereotactic conformal irradiation, which is characterized by submillimeter accuracy of dose delivery and high selectivity with a significant reduction of the impact on the surrounding normal structures[49,56]. Radiotherapy was performed on the Novalis device. In the patients' cohort that we have selected, the tumor location was such that the hippocampus, positioned in the immediate vicinity of the tumor, unavoidably fell into the radiation exposure zone (an example of such localization and the characteristics of the radiation treatment are in Fig. 1A,B,C). Patients received radiation treatment (total focal dose of 54 Gy) in the standard fractionation mode in 30 fractions (5 fractions each week). There were no statistically significant differences between the tumLeft and tumRight groups in the volume of the

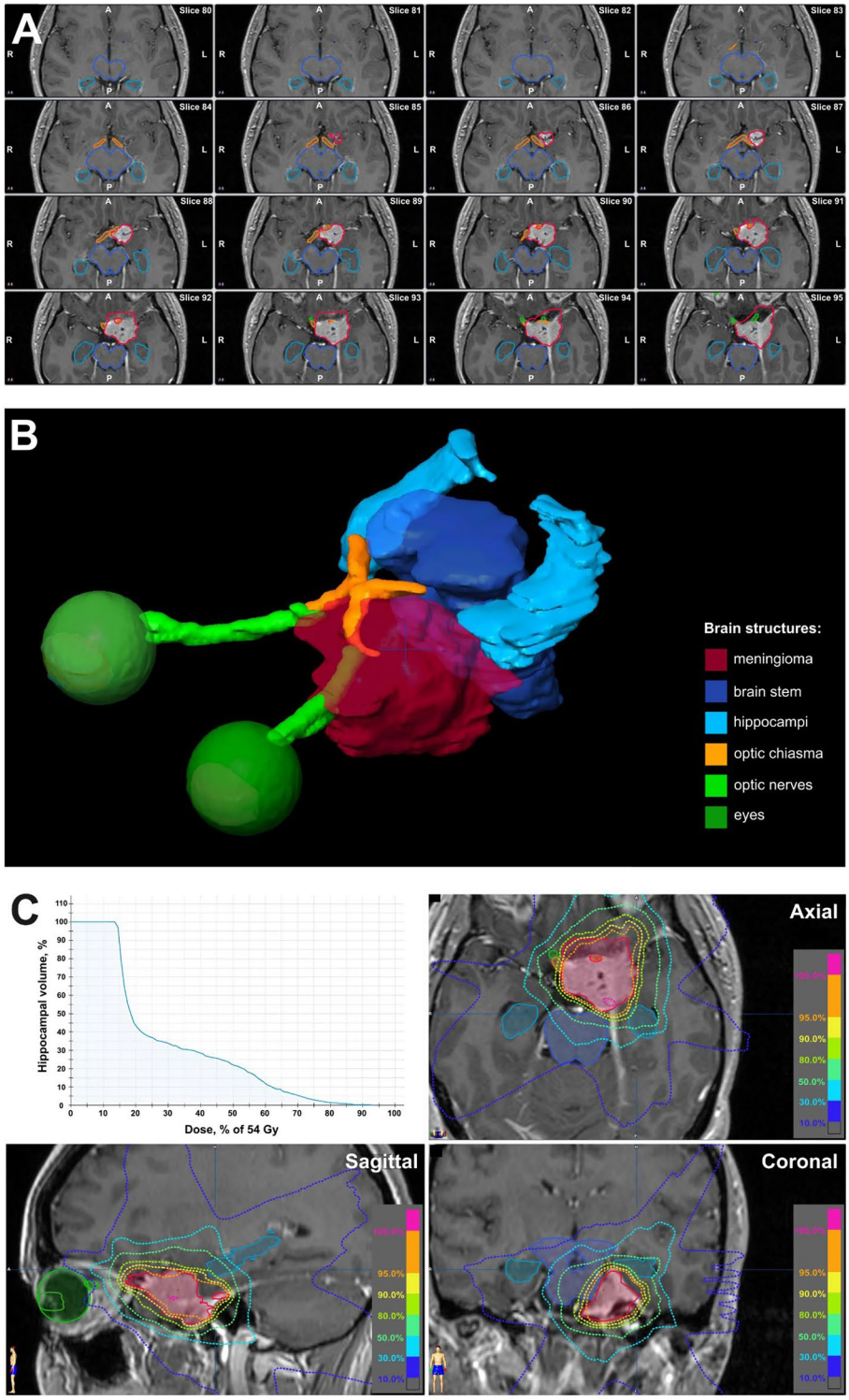

Fig. 1. Focal stereotactic radiotherapy of a meningioma tumor. (**A**) Axial tomograms in T1 mode with contrast enhancement of the patient's meningioma tumor. The area of the meningioma and key brain structures are highlighted in different colors (see the color chart legend in **B**). (**B**)Three-dimensional reconstruction of the tumor, the hippocampi, and the adjacent structures. (**C**) The irradiation dose distribution over the brain: the "dose-volume" histogram for one representative hippocampus reflecting what volume of the structure in % receives a certain dose in % of the prescribed dose (54 Gy). Tumor, hippocampi, and critical structures are outlined on T1 mode MRI tomograms in three projections (axial, frontal, and sagittal). The dose distribution is marked with dotted isodose lines. Each isoline outlines the region that received the same radiation dose, as a percentage.

tumor, of the ipsi- and contralateral hippocampi, or in the radiation doses received by the ipsi- or contralateral hippocampi (Supplementary Tables 1 and 2).

Timepoints and basic neuropsychological tests

Patients underwent neuropsychological and psychophysiological assessment at the following timepoints: (1) prior to treatment (0 months, the baseline), (2) immediately following the treatment (i.e., ~ 1.5 months after the therapy onset), and (3) 6 months, (4) 12 months, and (5) 24 months after the start of radiation therapy. The control group was subjected to identical tests at 0 and 1.5 months (corresponding to the beginning and the end of the radiation treatment of the meningioma patients). The test panel included standard protocols for evaluating cognitive status, such as the Wechsler Memory Scale, the dichotic listening test, the finger tapping test, and the bell test. Participants also completed a modified version of MST, designed to assess potential laterality effects on pattern separation and pattern completion (see next section). Furthermore, patients were analyzed for the changes in the tumor growth using MRI and for the clinical dynamics of neurological symptoms.

Modified MST design

MST[24,26–28,57] is based on presenting participants, in the first (encoding) phase of the task, with a series of individual images, and in the second (recognition) phase, of a series of images that are either identical, similar, or different from those shown previously. We modified the MST paradigm in order to detect potential differences associated with the left and right location of the tumor and the left vs. right presented visual stimuli. Specifically, after being instructed on the details of the test, each subject was sequentially presented on the monitor screen with triplets of images arranged in horizontal rows. Each triplet presentation lasted for 10 s and was interspersed with the presentation of a gray screen without images, to minimize carry-over visual effects. Ten minutes after the end of the encoding phase, participants were asked to recall, in a random order, the images they had seen ("free recall"). Twenty minutes later (i.e., thirty minutes after the triplets' presentation), during the testing phase, they were shown a new series of images, this time presented individually. This new series included (a) the same images that were presented in the encoding phase ("targets"); (b) images slightly different from the presented images in detail, color, or perspective ("lures"); and (c) images entirely different from the originally presented images ("foils"). In addition, the distribution of attention by the subjects was assessed by registering the eye movement[58], performed in parallel with the MST. Eye-tracking[58,59] showed that in all subjects the duration of gaze fixation in the central part of the triplet was higher than in the lateral sectors; however, there was no significant difference in the duration and distribution of gaze fixation in the lateral parts of the screen (i.e., left- and right-presented visual stimuli).

For each image, the subjects were asked to characterize it as (a) those that they had seen previously ("old"); (b) bearing a resemblance to the original images but not identical to them ("similar"); or (c) as images that were not presented earlier ("new"). Responses were recorded and categorized into nine possible outcome types (e.g., target/old, target/new, target/similar, etc.) (Fig. 2). The distribution of the responses (i.e., percentage endorsed for each stimulus and each response type) indicated that the mnemonic similarity of the stimuli, lures in particular, was sufficient for generating a representative range of possible participants' responses (for instance, 31.2% for "lure/old", 59.9% for "lure/similar", and 8.9% for "lure/new") (Supplementary Table 3).

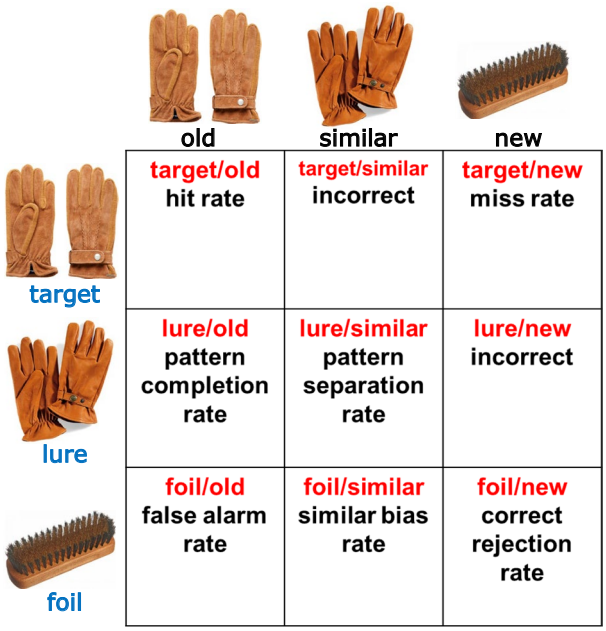

Fig. 2. Design of the experiments: the images presented to the subjects during the encoding and the recognition phases, and a schematic table of potential responses and the parameters used to determine the bias-corrected recognition, pattern separation, and pattern completion.

Free recall

Ten minutes after the last image triplet presentation, subjects were asked to recall, in any order, the images shown to them on the screen during encoding. The proportion of correctly recalled was presented as the "free recall" score (Fig. 3A).

There were no statistically significant differences in free recall accuracy before the start of the treatment (baseline) for the groups with left or right localization of the tumor (tumLeft and tumRight groups) and the healthy controls, and the recall rates fell within a normative range for this test[58,59]. Throughout the observation period there was no significant difference across the timepoints (0, 1.5, 6, 12 and 24 months) (effect of timepoint F (4, 119) = 1.914, $P = 0.1126$), between the groups with left vs. right localization of the tumor (tumLeft and tumRight) (effect of tumor localization F (1, 119) = 0.000, $P > 0.999$), or for the left- and right-positioned visual stimuli in the triplet in either tumLeft or tumRight group (Fig. 3A) (Supplementary Table 4a, line 1). This indicates that the participants' ability to recall the stimuli was not affected by the presence of the tumor prior to irradiation treatment or by the treatment itself.

Recognition memory

Among the parameters that can be derived from the MST results, is a measure of recognition memory performance, the bias-corrected recognition memory index[24], determined here as the proportion of targets correctly identified as "old" (target/old) minus the proportion of foils incorrectly endorsed as "old" (foil/old).

We did not detect any differences in recognition memory between the tumLeft and tumRight groups at any of the tested timepoint (Fig. 3B, effect of timepoint F (4, 119) = 0.5331, $P = 0.7116$). Likewise, we did not observe differences between the tumLeft, tumRight, and control groups at baseline (prior to treatment), nor between left- and right-positioned visual stimuli in the triplet in either tumLeft or tumRight group at any timepoint (Supplementary Table 4a, line 2). These results are consistent with the results of the free recall measurements (Fig. 3A), supporting the conclusion that neither the initial presence of the tumor nor the subsequent irradiation altered the basic ability of the subjects to remember the stimuli.

Pattern separation

We next determined participants' capacity for pattern separation, defined as the fraction of lures correctly recognized as "similar" (lure/similar) minus the fraction of foils incorrectly endorsed as "similar" (foil/similar) and presented as bias-corrected pattern separation index (BPS)[24,26]. There was no significant difference in BPS scores between the tumLeft, tumRight, and control groups before the start of treatment, indicating that the presence of the tumor did not affect the BPS capacity on its own (Fig. 4A, Supplementary Table 4a, lines 3–4).

However, there were important differences in the time course of changes in the tumRight group (Fig. 4A): while there was no significant difference between the first three timepoints (0, 1.5, and 6 months), a significant decrease in the BPS score was observed 12 months after the start of treatment, compared to both pre-treatment

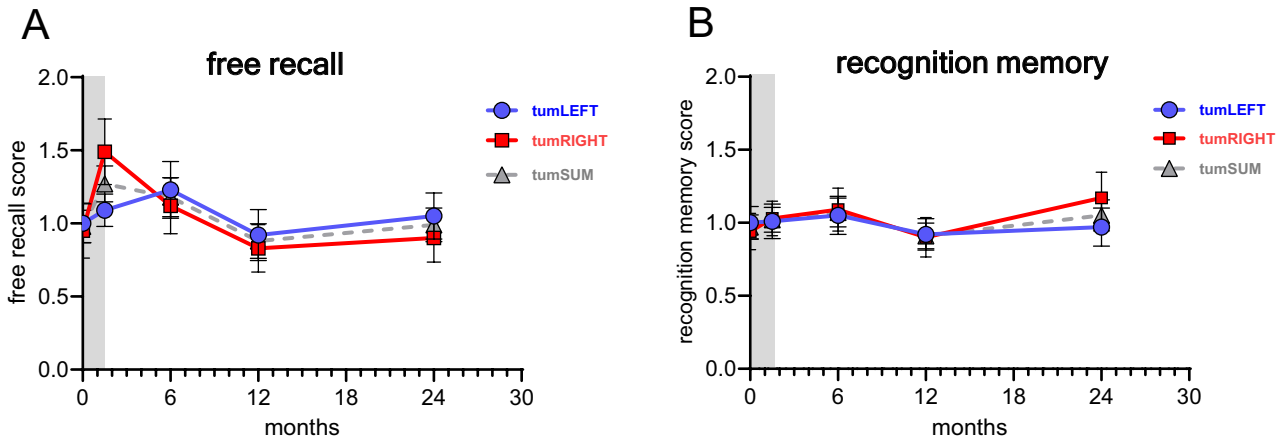

Fig. 3. Free recall (**A**) and recognition memory (**B**). (**A**) Free recall score was determined as the fraction of correctly remembered images presented on the screen 10 min earlier. The data are normalized to the results at the 0 month timepoint of the tumLeft group. No statistically significant differences were detected for the tumLeft and tumRight data, both between and within the groups, during the course of analysis, or in comparison with the performance immediately before the irradiation treatment. The grey bar here and in subsequent figures marks the time period of irradiation (1.5 months). For statistical analysis, see Supplementary Table 4a (line 1). (**B**) Bias-corrected recognition memory score (BPR) was determined as the fraction of the already presented images (targets) correctly recognized as such (target/old) minus the fraction of the images never presented to the subject (foils) but incorrectly recognized as already presented (foil/old). The data are normalized to the results at the 0-month timepoint of the tumLeft group. No statistically significant differences were detected for the tumLeft and tumRight, both between and within the groups, during the course of analysis or in comparison with the performance immediately before the treatment. For statistical analysis, see Supplementary Table 4a (line 2).

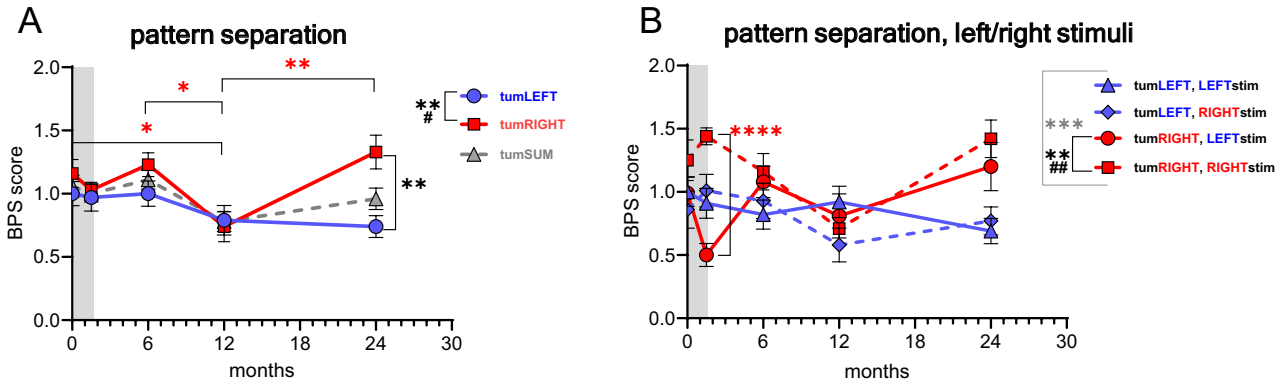

Fig. 4. The dynamics of changes in bias-corrected pattern separation (BPS). (**A**) BPS score was determined as the fraction of the images similar but not identical to those already presented (lures) correctly recognized as similar (lure/similar) minus the fraction of the images never presented to the subject but incorrectly recognized as similar (foil/similar). The data are normalized to the results at the 0-month timepoint of the tumLeft group. Note that in the tumRight group, the score was decreased after 12 months and restored after 24 months; no statistically significant differences were detected for the tumLeft or the tumSum groups over the entire course of analysis. The overall dynamics of changes over the course of analysis were different for the tumLeft and tumRight groups. Red asterisks correspond to tumRight data. Vertical black bracket and asterisks at t = 24 months correspond to the comparison between the tumRight and tumLeft groups at that timepoint. Vertical black bracket and symbols in the chart legend correspond to the comparisons between tumor localizations (*) and across timepoints (#). $^{*}p \le 0.05$, $^{**}p \le 0.01$, $^{\#}p \le 0.05$. For statistical analysis, see Supplementary Table 4a (lines 3–4). (**B**) BPS score was determined separately for the stimuli presented on the right or on the left for the tumLeft and tumRight groups (marked as, e.g., tumLeft, Left stim). The data are normalized to the tumLeft/Left stimuli results at the 0-month timepoint. Note a high difference for the tumRight/Left stimuli and tumRight/Right stimuli results at the 1.5-month timepoint (black bracket, red asterisks in the chart), which corresponds to the end of the irradiation sessions. Vertical black bracket and symbols in the chart legend correspond to the comparisons between the stumulus localization (*) and across timepoints (#). Grey brackets and grey asterisks in the chart legend refer to the comparison across timepoints between all four sets of resutls. $^{**}p \le 0.01$, $^{***}p \le 0.001$, $^{****}p \le 0.0001$, $^{\#\#}p \le 0.01$. For statistical analysis, see Supplementary Table 4a (lines 5–7).

baseline (q = 3.919, $P = 0.0498$) and 6 months scores (q = 4.573, $P = 0.0135$). Importantly, this decrease was transient: by 24 months, the BPS score had returned to baseline levels, with a significant difference between the 12- and 24-month timepoints (q = 4.854, $P = 0.0072$), but no significant difference between the 0- and 24-month timepoints.

Remarkably, the observed changes were specific to the tumRight group: no statistically significant BPS changes were revealed in the tumLeft group at any timepoint in comparison with any other timepoint; furthermore, there was significant difference between the tumRight and tumLeft groups in the overall trajectories of changes and the 24-month timepoint values (t = 3.549, $P = 0.0028$) (Fig. 4A). Notably, when data from both tumor groups were pooled (i.e., under the design similar to the conventional version of MST), the difference between the timepoints across the time-course of the study was not detectable (grey line in Fig. 4A).

Together, these results indicate that in the tumRight group, the capacity for pattern separation declined by 12 months post-irradiation, but was restored to the original levels by 24 months. No comparable difference was observed in the tumLeft group across the entire time-course of the study.

Pattern separation for the left- and right-presented visual stimuli

We next examined subjects' capacity for pattern separation in relation to the side of the presented stimuli (the images on the left or on the right side of the triplet, i.e., ipsi- or contralateral to the tumor). In the tumRight group, BPS scores showed significantly different overall dynamics of changes for the left- versus right-presented stimuli (effect of timepoint F (4, 106) = 3.855, estimated effect size $\eta^2 = 0.1012$, $P = 0.0058$; effect of stimulus localization F (1, 106) = 10.10, estimated effect size $\eta^2 = 0.0668$; $P = 0.0019$, interaction F (4, 106) = 4.480, $P = 0.0022$; Supplementary Table 4a, lines 5–6, Supplementary Table 4b, line 1) (Fig. 4B). There was also a highly significant threefold difference in the BPS score for the left- and right-sided stimuli in the tumRight group at the 1.5-month timepoint (i.e., the timepoint corresponding to the end of radiation exposure phase), the score being lower for the left-sided stimuli, i.e., contralateral to the location of the tumor (t = 5.142, $P < 0.0001$) (Fig. 4B). The difference between the left- and right-presented stimuli in the tumRight group was resolved by the 6-month timepoint and was not observed later.

In contrast, patients in the tumLeft group did not exhibit any bias for the contra- or ipsi-lateral-presented stimuli throughout the time-course of the study (effect of timepoint F (4, 132) = 1.350, estimated effect size $\eta^2 = 0.0379$, $P = 0.2547$, effect of stimulus localization F (1, 132) = 0.2288, estimated effect size $\eta^2 = 0.0016$,

$P = 0.6332$), and there was a highly significant difference between the overall dynamics of changes in the tumLeft and tumRight groups with right- or left-presented stimuli (Fig. 4B).

These results reveal a remarkable difference in pattern separation in response to the stimuli presented ipsi- and contralaterally to the tumor location for the tumRight group 1.5 months after the start of treatment. Of note, this timepoint corresponds to the end of the radiation exposure, i.e., the period when the targeted region shows signs of inflammation, possibly reflecting massive cell death in the vicinity of the irradiated tumor.

Pattern completion

We next assessed participants' capacity for pattern completion, defined as the fraction of lures incorrectly endorsed as "old" (lure/old) minus the fraction of foils incorrectly endorsed as "old" (foil/old) and presented as bias-corrected pattern completion index (BPC)[24,26].

As with the pattern separation measurements, there was no significant difference in BPC scores between the tumLeft, tumRight, and control groups before the start of treatment, indicating that the presence of the tumor on its own did not affect the capacity for pattern completion (Fig. 5A). However, there was a significant difference in the overall time-courses of changes between the tumLeft and tumRight groups (effect of timepoint $F(4,119) = 5.036$, $P = 0.0009$) (Fig. 5A). There was also a significant difference in the trajectories of changes within the tumLeft or tumRight groups (effect of tumor localization $F(1,119) = 9.005$, $P = 0.0033$). The tumRight group showed particularly pronounced changes, with differences between the 0- and 12-month ($q = 3.940$, $P = 0.0479$), 6- and 12-month ($q = 4.828$, $P = 0.0077$), and 12- and 24-month timepoints ($q = 4.697$, $P = 0.0103$), indicating a significant bias towards pattern completion 12 months after the beginning of treatment. Similar to BPS, the peak at 12 months was transient, with no difference between the 0-, 1.5-, or 6-month vs. the 24-month timepoints, suggesting that by 24 months the BPC score returned to the baseline pre-treatment values.

The kinetics was different for the tumLeft group, where the capacity for pattern completion showed an increase by 12 months ($q = 4.020$, $P = 0.0413$) but did not decrease by 24 months post-irradiation (however, the difference with the start point was not significant). As with the BPS scores, these differences were not detectable when data from both tumor groups were combined (grey line in Fig. 5A), underscoring the importance of laterality-specific analysis.

Together, these results indicate that in the tumRight group the capacity for pattern completion peaked by 12 months post-irradiation, but was restored to the original levels by 24 months.

Pattern completion for the left- and right-presented visual stimuli

Next, paralleling the BPS measurements, we analyzed participants' capacity for pattern completion in relation to stimulus laterality (i.e., left- or right-presented images) (Fig. 5B, Supplementary Table 4a, lines 9–10,

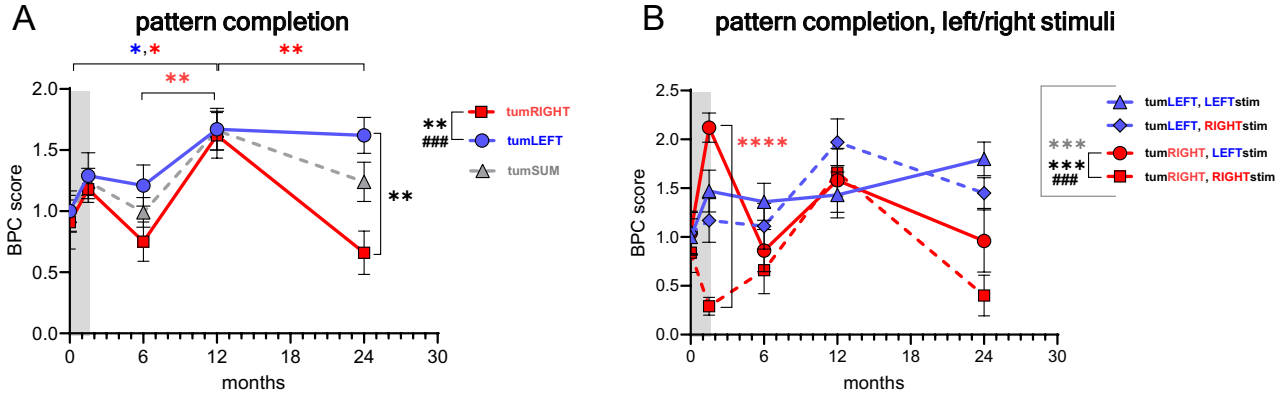

Fig. 5. The dynamics of changes in bias-corrected pattern completion (BPC). (**A**) BPC score was determined as the fraction of the images similar but not identical to those already presented (lures) incorrectly recognized as already presented (lure/old) minus the fraction of the images never presented to the subject but incorrectly recognized as already presented (foil/old). The data are normalized to the results at the 0-month timepoint of the tumLeft group. Note that in the tumRight group, the score was increased after 12 months and restored after 24 months. Red and blue asterisks correspond to tumRight and tumLeft data, respectively. Vertical black bracket and asterisks at t = 24 months correspond to the comparison between the tumRight and tumLeft groups at that timepoint. Vertical black bracket and symbols in the chart legend correspond to the comparisons between the tumor localizations (*) and across timepoints (#). $^{*}p \le 0.05$, $^{**}p \le 0.01$, $^{\#\#\#}p \le 0.001$. For statistical analysis, see Supplementary Table 4a (lines 8–9). (**B**) BPC score was determined separately for the stimuli presented on the right or on the left for the tumLeft and tumRight groups. The data are normalized to the tumLeft/Left stimuli results at the 0 timepoint. Note a high difference for the tumRight/Left stimuli and tumRight/Right stimuli at the 1.5-month timepoint (black bracket, red asterisks), which corresponds to the end of the irradiation sessions. Vertical black bracket and symbols in the chart legend correspond to the comparisons between the stimulus localization (*) and across timepoints (#). Grey brackets and grey asterisks in the chart legend refer to the comparison across timepoints between all four sets of results. $^{***}p \le 0.001$, $^{****}p \le 0.0001$, $^{\#\#\#}p \le 0.001$. For statistical analysis, see Supplementary Table 4a (lines 10–12).

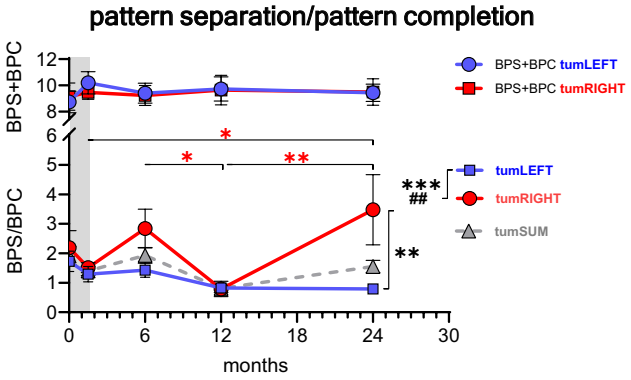

Fig. 6. The dynamics of changes in the relation between BPS and BPC. The ratio of the BPS to BPC scores was determined for each timepoint for the tumLeft, tumRight, and tumSum groups (the lower part of the graph). The upper part of the graph shows the sum of the tumLeft and tumRight scores, which does not change over the entire course of analysis. Red asterisks correspond to tumRight data. Vertical black bracket and asterisks at t = 24 months correspond to the comparison between the tumRight and tumLeft groups at that timepoint. Vertical black bracket and symbols in the chart legend correspond to the comparisons between the tumor localizations (*) and across timepoints (#). $^{*}p \le 0.05$, $^{**}p \le 0.01$, $^{***}p \le 0.001$, $^{\#\#}p \le 0.01$. For statistical analysis, see Supplementary Table 4a (lines 13–14).

Supplementary Table 4b, line 2). In the tumRight group, there was a highly significant difference in BPC score trajectories for the left vs. right-presented stimuli (effect of timepoint F (4, 106) = 5.423, estimated effect size $\eta^2 = 0.1285$, $P = 0.0005$, effect of stimulus localization F (1, 106) = 14.31, estimated effect size $\eta^2 = 0.0848$, $P = 0.0003$, interaction F (4, 106) = 6.275, $P = 0.0001$); there was also a highly significant difference between the overall dynamics of changes in regard to the stimuli in the tumLeft and tumRight groups (Fig. 5B). As with BPS, the lateralized difference was particularly pronounced (> sevenfold difference; t = 6.155, $P < 0.0001$) at the end of radiation exposure phase (the 1.5-month timepoint), with higher BPC scores for left (contralateral) stimuli (Fig. 5B).

Paralleling the BPS results, the subjects with left-localized tumors did not demonstrate a bias in BPC for the left or right stimuli throughout the course of treatment (Fig. 5B), and the scores for the stimuli presented at either side at the last (24-month) timepoint returned to the pre-treatment values.

Ratio of BPC to BPS

We next addressed the relationship between pattern completion and pattern separation by determining the time course of changes in the BPC/BPS ratios. There were drastic changes in the ratio as a function of time after irradiation, the difference reaching 2.8-fold 6 months after irradiation and 3.3-fold 24 months post-irradiation, but approaching the value of one by 12 months, with a highly significant difference between the overall dynamics of changes in the tumLeft and tumRight groups (effect of timepoint F (4, 117) = 3.500, $P = 0.0098$) (Fig. 6, lower part). However, the sum of BPS and BPC scores remained stable throughout the observation period (effect of timepoint F (4, 117) = 0.3437, $P = 0.8480$) (Fig. 6, upper part), suggesting a dynamic trade-off between these processes rather than a net loss in overall performance. These results are consistent with the time courses of two complementary error metrics—target/new responses ("miss rate"), and foil/old responses ("false alarm rate"), which remained stable across timepoints for both tumor groups.

Together, these results indicate that while the balance between pattern separation and pattern completion shifted during the post-irradiation period, the overall capacity to perform these cognitive operations remained intact over the full 24-month follow-up period. These observations are also consistent with the results of the free recall and recognition memory measurements (Figs. 3A,B), supporting the conclusion that the overall capacity for remembering the stimuli was not affected by the presence of the tumor or the subsequent irradiation.

Discussion

Our results describe changes in several aspects of learning and memory in a cohort of patients with extracerebral tumors located adjacent to the hippocampi who underwent prolonged fractionated irradiation, using a targeted beam that also affected the hippocampi on the side of the irradiated tumor. Our findings suggest that focal irradiation of the human hippocampus, which most likely entails a targeted elimination of dividing neural progenitors in the DG, does not affect the basic parameters of learning and memory, but selectively impacts complex cognitive operations such as pattern separation and pattern completion.

Specifically, patients with tumors adjacent to the hippocampus did not exhibit evident deficits in standard measures of memory such as free recall or recognition memory or other basic parameters of the cognitive status throughout the two-year observation period; notably, the hippocampal volume did not change during that period.

However, 12 months after the start of irradiation, distinct changes emerged in more nuanced hippocampal-dependent functions: patients with right-sided tumors showed a significant decline in pattern separation and an

increase in pattern completion. Importantly, 24 months after irradiation, the BPS and BPC scores returned close to the original levels in both groups. Nonetheless, at the 24-month timepoint, patients with right-sided tumors exhibited significantly higher BPS and lower BPC scores compared to those with left localization of the tumor, confirming differentially altered MST performance following irradiation, dependent on tumor localization.

Together, our results reveal a marked effect of laterality in patients' capacity for pattern separation and pattern completion following irradiation,—presumably under conditions of irradiation-suppressed hippocampal neurogenesis. Of note, the time-dependent changes in pattern separation and pattern completion were only marginally evident when the results from the right- and left-irradiated groups were combined, underscoring the importance of a targeted initial study design that accounts for potential hemisphere asymmetry after focal intervention and allows for the detection of such left/right bias.

The remarkable difference between the BPS and BPC trajectories in the left- and right-irradiated patient subcohorts agrees well with the vast body of evidence that the right hemisphere and the right hippocampus are particularly important for tasks relying on visuospatial memory, in contrast to the left hemisphere, which is more closely related to the processing of verbal signals[50,51,55]. This functional asymmetry is evident both in the deterioration and in subsequent recovery of BPS and BPC scores in the right-irradiated subcohort (cf. values for 12- and 24-month post-irradiation analysis).

Notably, we also observed a different type of laterality, manifested as a significant difference in the processing of visual stimuli presented ipsi- versus contra-lateral to the location of the tumor (and hence, the irradiated side of the brain). Specifically, in the right-irradiated cohort, there was a 3- and sevenfold difference, respectively, in the number of pattern separation and pattern completion errors related to stimuli presented on the left (i.e., contralateral to the tumor) compared to the stimuli on the right. These findings are consistent with evidence of deficits in processing visual fields contralateral to the affected hemisphere under competition from symmetrical stimuli[60]. Interestingly, the difference between the left- and right-presented stimuli was most pronounced at 1.5 months after the start of irradiation, coinciding with the end of treatment when a significant number of tumor cells die and are cleared from the tissue, leading to an inflammatory response and local edema. This may indicate that the inter-visual field difference is most pronounced when the hippocampal tissue is stressed by the inflammatory response in its vicinity and may decrease as the inflammatory processes subside. Note, however, that other analyzed parameters, such as free recall and recognition memory, were not significantly affected at this timepoint compared to the preceding (0-month) or following (6-, 12-, or 24-month) timepoints, supporting the specificity of the observed changes. Furthermore, as per MRI results, the entire group of patients did not show signs of neuroinflammation at the later timepoints (6-, 12-, or 24-month).

Crucially for the conclusions of this study, the results cannot be attributed to pre-existing differences in BPS or BPC, as there were no significant differences in these parameters before the start of irradiation treatment (i.e., at the 0-month timepoint) between both the tumor patients' and control (subjects without a tumor) groups. Additionally, the results cannot be explained by the uneven distribution of attention to the left vs. right stimuli, as evidenced by the eye-tracking data.

Our findings indicate that the BPS/BPC ratio varies significantly during the course of analysis, with clear inter-hemispheric differences, supporting the notion that while pattern separation and pattern completion are conceptually related and, in this study design, experimentally linked, they do not simply mirror each other, but instead follow distinct temporal trajectories that also reflect tumor laterality. This is consistent with their close, but not fully reciprocal, functional roles (encoding for pattern separation and retrieval for pattern completion) and their neuroanatomical basis (e.g., the importance of the DG for pattern separation and of CA3 for pattern completion)[8–10]. It should be emphasized, however, that the involvement of DG and CA3 in the two processes has been shown as a crucial, but not as a sufficient, input, and in the live brain, the entire entorhinal cortex-DG-CA3-CA1 axis may be important for both pattern separation and pattern completion[1,7,8,10–12].

Notably, the sums of BPS and BPC remain stable throughout the observation period, compatible with the constant levels of the "miss rate" and "false alarm" errors as well as free recall and recognition memory scores in the irradiated patients. Taken together, our results indicate that the overall capacity for memory discrimination and generalization, as revealed in the tests for pattern separation and pattern completion, did not suffer during the 2 years of treatment and observation.

Although the persistence of hippocampal neurogenesis in the adult human brain remains debated[31,61–63], recent reports provide multipronged evidence for its continuation in adult humans and primates, albeit with kinetics significantly slower than that in rodents[30,33,34,53,64–67]. In particular, our results are consistent with those that describe changes in the human brain affected by aging and Alzheimer's disease[29,32], the RNA expression patterns of human neural progenitors[34,54], and the slow maturation of human neurons grown as organoids[52].

A plausible interpretation of our results is that focal irradiation impairs local production and integration of newborn neurons in the adult DG. We posit that while radiation damages and eliminates dividing neural stem and progenitor cells, their deficit is not reflected in behavioral tests at earlier stages (up to 6 months). However, by 12 months, the reduced supply of new neurons may begin to compromise behavioral responses requiring efficient pattern separation and pattern completion. These deficits could be mitigated over time by the gradual maturation of the neuronal progenitors, which eventually reach functional maturity and fulfill their roles in BPS and BPC (also note that in the animal brain irradiation, besides eliminating actively dividing cells, leads to a temporary suppression of the activity of neural stem cells that have survived irradiation[39]).

While there is a vast body of evidence potentially linking pattern separation and adult neurogenesis in humans, much of it concerns comparisons between different groups of subjects (e.g., with and without mild cognitive impairment, Alzheimer's disease, trauma, or seizures) [24,26,28,57]. Ours is the first longitudinal study to monitor changes in memory, pattern separation, and pattern completion within the same patient cohort over two years, revealing a defined time-course of deterioration and recovery of pattern separation and pattern completion within the same subjects. Also important for the conclusions of the study, meningiomas are extracerebral tumors

and do not alter or infiltrate the neural tissue *per se*, as in the case of brain tumors, brain metastasis, neurological disorders, and trauma; therefore, unavoidable elimination of dividing neural progenitors by irradiation arises as a plausible explanation of our results. Taken together, our results provide support for the importance of ongoing hippocampal neurogenesis in specific cognitive operations in humans.

While our study offers experimentally-supported conclusions on the potential link between damage to the hippocampus and altered pattern separation and pattern completion performance, there are several limitations and caveats to consider. In particular, in the absence of the ability to directly measure neurogenesis in the living human brain, our study provides correlative, rather than direct, evidence that the neurogenic function of the hippocampus is responsible for the pattern separation and pattern completion deficits observed after irradiation. Indeed, it is conceivable that the defects we observe are due, at least partially, to impairments in other functions of the hippocampus or DG, unrelated to neurogenesis[7,11,12,46,47,68]. Such defects may include vascular injury, microstructural white matter changes, and local inflammation[46,47]. Furthermore, the observed changes may also be induced by network-level plasticity and reorganization (e.g., compensatory recruitment of the contralateral or extra-hippocampal networks). Nevertheless, since the elimination of dividing cells is a primary consequence of radiation exposure, its effect on neurogenesis should be considered among the main potential explanations for the observed changes. Furthermore, the high specificity of the observed changes (e.g., intact free recall and recognition memory) supports the interpretation that radiation-induced alterations in neurogenesis specifically underlie the observed deficits in pattern separation and pattern completion.

Furthermore, our study design precludes the inclusion of an "ideal" control group beyond the pre-exposure tests (when the conditions for the control and trial groups can be matched), as the patients undergo a lengthy (1.5 months) series of psychologically and physiologically demanding therapeutic procedures that cannot be applied to a control group (e.g., immobility, head fixation, and inevitable stress and anxiety related to the disease and surgery). However, we consider the longitudinal design of the analysis of the same subjects as outweighing the lack of direct comparisons with control groups at the post-exposure stages of the study.

One additional consideration is that the hippocampus contralateral to the irradiation site still received a dose of radiation, even though it was significantly lower than that received by the ipsilateral hippocampus (Supplementary Table 2); still, our results indicate a marked difference between the responses of the left- and right-irradiated groups.

Regardless of the mechanistic basis for the observed changes, our findings carry several clinical implications. First, they highlight the need to evaluate potential cognitive side effects when planning radiation treatment in patients with tumors located adjacent to the hippocampus and suggest that strategies to preserve or restore hippocampal neurogenesis should be considered when designing treatments for brain tumors and other neurological conditions. Second, they provide further support for the use of MST and its modifications in evaluating the fine aspects of learning and memory in humans. Finally, our study provides a framework for future research exploring the mechanisms of pattern separation and pattern completion in humans and their connection to hippocampal neurogenesis.

Materials and methods

Participants

The study included 28 patients (24 females and 4 males of median age 52 ± 10.7 years) with cavernous sinus meningiomas situated either to the left or right of the optic chiasm and adjacent to the hippocampus. Detailed characteristics of the patient group—including age, sex, education, handedness, visual acuity, oculomotor function, tumor volume and localization, and the volumes of the hippocampus ipsilateral and contralateral to the tumor—are provided in Supplementary Table 1. None of the participants had previously undergone radiotherapy or neurosurgical intervention and all participants were screened for medical conditions that could affect neurological assessment. The control group consisted of 29 healthy individuals (23 females and 6 males, with median age of 49.3 ± 12.2 years), matched to the clinical groups by age, sex, and education level. The criterion for not including healthy subjects in the group was a history of craniocerebral trauma, strokes, observation by a neurologist or psychiatrist, or taking psychotropic drugs. Due to the clinical and organizational restrictions and decreased compliance during the COVID-19 pandemic, part of the control group was not investigated at the later (6-, 12-, 24-month) timepoints. Also note that some of the radiation therapy-related procedures applied to the patients (e.g., head fixation and immobility for prolonged periods of time) cannot be applied to the subjects in the control group, thus making the measurements beyond the pre-exposure (0-month) timepoints less informative.

The patients were tested in MST as a part of the neurological and psychological assessment when they visited the clinic at defined periods of time post-therapy to be evaluated for the changes in the tumor growth using MRI and for the clinical dynamics of neurological symptoms. The study was observational, as in the course of this study, we only collected the data on the patients' neurological and neuropsychological status, without actively intervening or manipulating the existing conditions. The study did not contradict clinical guidelines and did not have a negative impact on the treatment results. The study was conducted in accordance with the principles of biomedical ethics as outlined in the 1964 Declaration of Helsinki and its later amendments. The study was approved by the Bioethics Committee of the Burdenko National Medical Research Center for Neurosurgery, Ministry of Health of Russia (Moscow), protocol no. 05 dated 2017. Each participant in the study provided a voluntary written informed consent after receiving an explanation of the potential risks and benefits, as well as the nature of the upcoming study.

Radiation therapy and neuropsychological assessment

All patients underwent topometric head magnetic resonance imaging (MRI): axial T2 images (slice thickness 2 mm) and axial three-dimensional spoiled gradient recalled acquisition in steady state (3D SPGR), enhanced

and non-enhanced (slice thickness 1 mm) before the treatment. For accurate volume estimation and dosimetry target and hippocampal contouring were performed in the iPlan planning system (BrainLab, Munich, Germany). Hippocampal contouring was performed according to the Radiation Therapy Oncology Group (RTOG) 0933 protocol. Treatments were performed in the radiotherapy department of the N.N. Burdenko National Medical Research Center of Neurosurgery, Moscow.

The meningioma patients' group underwent stereotactic conformal radiation therapy with a photon beam using the Novalis linear accelerator (Varian, BrainLab) (6 MeV) equipped with a micromultileaf collimator. Radiotherapy was delivered in the standard fractionation scheme in 30 fractions (5 fractions per week), with a single dose of 1.8 Gy and a total focal dose of 54 Gy (Fig. 1A,B). This procedure resulted in an average radiation exposure of 40.0 Gy, 29.3 Gy, and 20.8 Gy for 10%, 30%, and 50%, respectively, of the volume of the hippocampus adjacent to the tumor. For the contralateral hippocampus, the average dose load of 10% 30% and 50% of the hippocampal volume was 13.8 Gy, 9.7 Gy, and 8.0 Gy, respectively (Fig. 1C, Supplementary Table 2). The patients in both groups (with left and right localization of tumor) received similar doses of radiation for the zone ipsilateral to the tumor ($p > 0.42$) or contralateral to the tumor ($p > 0.67$) (Supplementary Table 2). Furthermore, there were no noticeable differences in tumor volume or position between the experimental groups.

Patients underwent a battery of neuropsychological tests that included the MST, specifically adapted to assess pattern separation and pattern completion. These tests were conducted immediately before (baseline, 0-month timepoint), and after (1.5-month timepoint) the radiation treatment, and at 6, 12, and 24 months after the start of treatment. As a result of the treatment, the last follow-up tumor growth stopped in 100% of cases, and a significant decrease in tumor volume was recorded in 33.3% of cases, according to MRI. The overall volumes of the ipsi- and contralateral hippocampi did not change during the course of observations (Supplementary Table 2).

Mnemonic similarity task (MST)

The basic design of MST[27,28] was modified in order to assess, besides pattern separation and pattern completion, the potential laterality effects relative to tumor position and visual stimulus presentation (additional details provided in the Results section). Briefly, after explaining the purpose and the details of the task, participants were shown triplets of images and asked to list the images 10 min later ("free recall"). This was followed, 30 min after the presentation of the images, by demonstration of a series of individual (i.e., not in triplets) images that were identical (targets), similar (lures), or dissimilar (foils) to those initially presented, and the participants were asked to categorize these images as "old", "similar", or "new". Performance metrics included the bias-corrected recognition score (BPR), bias-corrected pattern separation score (BPS), and bias-corrected pattern completion score (BPC), as defined in the Results. In parallel, eye movement and duration of gaze fixation for the central, left, and right visual stimuli was monitored[58,59].

Statistics

The data were analyzed and the graphs were generated using the GraphPad Prism 10 program (GraphPad Software LLC, USA). For convenience, full statistical data and behavioral characteristics are presented in Supplementary Tables 4a-c, with the key differences indicated in the figure panels.

Data availability

The datasets used and analyzed during the current study are available from the authors (O.A.K., M.V.G., and G.E.) on reasonable request.

Received: 16 September 2025; Accepted: 19 November 2025
Published online: 15 December 2025

References

1. Leal, S. L. & Yassa, M. A. Integrating new findings and examining clinical applications of pattern separation. *Nat Neurosci* **21**, 163–173. https://doi.org/10.1038/s41593-017-0065-1 (2018).
2. Yassa, M. A. & Stark, C. E. Pattern separation in the hippocampus. *Trends Neurosci* **34**, 515–525. https://doi.org/10.1016/j.tins.2011.06.006 (2011).
3. Aimone, J. B., Deng, W. & Gage, F. H. Adult neurogenesis: integrating theories and separating functions. *Trends Cogn Sci* **14**, 325–337 (2010).
4. Aimone, J. B., Deng, W. & Gage, F. H. Resolving new memories: a critical look at the dentate gyrus, adult neurogenesis, and pattern separation. *Neuron* **70**, 589–596. https://doi.org/10.1016/j.neuron.2011.05.010 (2011).
5. Sahay, A., Wilson, D. A. & Hen, R. Pattern separation: A common function for new neurons in hippocampus and olfactory bulb. *Neuron* **70**, 582–588. https://doi.org/10.1016/j.neuron.2011.05.012 (2011).
6. Johnston, S. T., Shtrahman, M., Parylak, S., Goncalves, J. T. & Gage, F. H. Paradox of pattern separation and adult neurogenesis: A dual role for new neurons balancing memory resolution and robustness. *Neurobiol Learn Mem* **129**, 60–68. https://doi.org/10.1016/j.nlm.2015.10.013 (2016).
7. Tuncdemir, S. N. et al. Adult-born granule cells facilitate remapping of spatial and non-spatial representations in the dentate gyrus. *Neuron* **111**, 4024–4039 e4027, https://doi.org/10.1016/j.neuron.2023.09.016 (2023).
8. Rolls, E. T. The mechanisms for pattern completion and pattern separation in the hippocampus. *Front Syst Neurosci* **7**, 74. https://doi.org/10.3389/fnsys.2013.00074 (2013).
9. Ngo, C. T., Michelmann, S., Olson, I. R. & Newcombe, N. S. Pattern separation and pattern completion: Behaviorally separable processes?. *Mem Cognit* **49**, 193–205. https://doi.org/10.3758/s13421-020-01072-y (2021).
10. Hunsaker, M. R. & Kesner, R. P. The operation of pattern separation and pattern completion processes associated with different attributes or domains of memory. *Neurosci Biobehav Rev* **37**, 36–58. https://doi.org/10.1016/j.neubiorev.2012.09.014 (2013).
11. Scharfman, H. E. & Myers, C. E. Corruption of the dentate gyrus by "dominant" granule cells: Implications for dentate gyrus function in health and disease. *Neurobiol Learn Mem* **129**, 69–82. https://doi.org/10.1016/j.nlm.2015.09.005 (2016).

12. Myers, C. E. & Scharfman, H. E. Pattern separation in the dentate gyrus: a role for the CA3 backprojection. *Hippocampus* **21**, 1190–1215. https://doi.org/10.1002/hipo.20828 (2011).
13. Aimone, J. B. et al. Regulation and function of adult neurogenesis: from genes to cognition. *Physiol Rev* **94**, 991–1026. https://doi.org/10.1152/physrev.00004.2014 (2014).
14. Deng, W., Aimone, J. B. & Gage, F. H. New neurons and new memories: how does adult hippocampal neurogenesis affect learning and memory?. *Nat Rev Neurosci* **11**, 339–350 (2010).
15. Lazutkin, A., Podgorny, O. & Enikolopov, G. Modes of division and differentiation of neural stem cells. *Behav Brain Res* **374**, 112118. https://doi.org/10.1016/j.bbr.2019.112118 (2019).
16. Ming, G. L. & Song, H. Adult neurogenesis in the mammalian brain: significant answers and significant questions. *Neuron* **70**, 687–702. https://doi.org/10.1016/j.neuron.2011.05.001 (2011).
17. Sahay, A. et al. Increasing adult hippocampal neurogenesis is sufficient to improve pattern separation. *Nature* **472**, 466–470 (2011).
18. Niibori, Y. et al. Suppression of adult neurogenesis impairs population coding of similar contexts in hippocampal CA3 region. *Nat Commun* **3**, 1253. https://doi.org/10.1038/ncomms2261 (2012).
19. Burghardt, N. S., Park, E. H., Hen, R. & Fenton, A. A. Adult-born hippocampal neurons promote cognitive flexibility in mice. *Hippocampus* **22**, 1795–1808. https://doi.org/10.1002/hipo.22013 (2012).
20. Clelland, C. D. et al. A functional role for adult hippocampal neurogenesis in spatial pattern separation. *Science* **325**, 210–213. https://doi.org/10.1126/science.1173215 (2009).
21. Tronel, S. et al. Adult-born neurons are necessary for extended contextual discrimination. *Hippocampus* **22**, 292–298. https://doi.org/10.1002/hipo.20895 (2012).
22. Danielson, N. B. et al. Distinct contribution of adult-born hippocampal granule cells to context encoding. *Neuron* **90**, 101–112. https://doi.org/10.1016/j.neuron.2016.02.019 (2016).
23. McAvoy, K. M. et al. Modulating neuronal competition dynamics in the dentate gyrus to rejuvenate aging memory circuits. *Neuron* **91**, 1356–1373. https://doi.org/10.1016/j.neuron.2016.08.009 (2016).
24. Stark, S. M., Yassa, M. A., Lacy, J. W. & Stark, C. E. A task to assess behavioral pattern separation (BPS) in humans: Data from healthy aging and mild cognitive impairment. *Neuropsychologia* **51**, 2442–2449. https://doi.org/10.1016/j.neuropsychologia.2012.12.014 (2013).
25. Yassa, M. A. et al. Pattern separation deficits associated with increased hippocampal CA3 and dentate gyrus activity in nondemented older adults. *Hippocampus* **21**, 968–979. https://doi.org/10.1002/hipo.20808 (2011).
26. Ally, B. A., Hussey, E. P., Ko, P. C. & Molitor, R. J. Pattern separation and pattern completion in Alzheimer's disease: evidence of rapid forgetting in amnestic mild cognitive impairment. *Hippocampus* **23**, 1246–1258. https://doi.org/10.1002/hipo.22162 (2013).
27. Stark, S. M., Kirwan, C. B. & Stark, C. E. L. Mnemonic similarity task: A tool for assessing hippocampal integrity. *Trends Cogn Sci* **23**, 938–951. https://doi.org/10.1016/j.tics.2019.08.003 (2019).
28. Stark, C. E. L., Noche, J. A., Ebersberger, J. R., Mayer, L. & Stark, S. M. Optimizing the mnemonic similarity task for efficient, widespread use. *Front Behav Neurosci* **17**, 1080366. https://doi.org/10.3389/fnbeh.2023.1080366 (2023).
29. Tobin, M. K. et al. Human hippocampal neurogenesis persists in aged adults and Alzheimer's disease patients. *Cell Stem Cell* **24**, 974–982 e973, https://doi.org/10.1016/j.stem.2019.05.003 (2019).
30. Moreno-Jimenez, E. P. et al. Adult hippocampal neurogenesis is abundant in neurologically healthy subjects and drops sharply in patients with Alzheimer's disease. *Nat Med* **25**, 554–560. https://doi.org/10.1038/s41591-019-0375-9 (2019).
31. Kempermann, G. et al. Human adult neurogenesis: Evidence and remaining questions. *Cell Stem Cell* **23**, 25–30. https://doi.org/10.1016/j.stem.2018.04.004 (2018).
32. Boldrini, M. et al. Human hippocampal neurogenesis persists throughout aging. *Cell Stem Cell* **22**, 589–599 e585, https://doi.org/10.1016/j.stem.2018.03.015 (2018).
33. Terreros-Roncal, J. et al. Impact of neurodegenerative diseases on human adult hippocampal neurogenesis. *Science* **374**, 1106–1113. https://doi.org/10.1126/science.abl5163 (2021).
34. Dumitru, I. et al. Identification of proliferating neural progenitors in the adult human hippocampus. *Science* **389**, 58–63. https://doi.org/10.1126/science.adu9575 (2025).
35. Schoenfeld, T. J., McCausland, H. C., Sonti, A. N. & Cameron, H. A. Anxiolytic Actions of Exercise in Absence of New Neurons. *Hippocampus* **26**, 1373–1378. https://doi.org/10.1002/hipo.22649 (2016).
36. Nokia, M. S., Anderson, M. L. & Shors, T. J. Chemotherapy disrupts learning, neurogenesis and theta activity in the adult brain. *Eur J Neurosci* **36**, 3521–3530. https://doi.org/10.1111/ejn.12007 (2012).
37. Shors, T. J. et al. Neurogenesis in the adult is involved in the formation of trace memories. *Nature* **410**, 372–376. https://doi.org/10.1038/35066584 (2001).
38. Encinas, J. M. et al. Quiescent adult neural stem cells are exceptionally sensitive to cosmic radiation. *Exp Neurol* **210**, 274–279. https://doi.org/10.1016/j.expneurol.2007.10.021 (2008).
39. Mineyeva, O. A. et al. radiation induces distinct changes in defined subpopulations of neural stem and progenitor cells in the adult hippocampus. *Front Neurosci* **12**, 1013. https://doi.org/10.3389/fnins.2018.01013 (2018).
40. Mizumatsu, S. et al. Extreme sensitivity of adult neurogenesis to low doses of X-irradiation. *Cancer Res* **63**, 4021–4027 (2003).
41. Monje, M. L., Mizumatsu, S., Fike, J. R. & Palmer, T. D. Irradiation induces neural precursor-cell dysfunction. *Nat Med* **8**, 955–962 (2002).
42. Rola, R. et al. Indicators of hippocampal neurogenesis are altered by 56Fe-particle irradiation in a dose-dependent manner. *Radiat Res* **162**, 442–446 (2004).
43. Rola, R. et al. High-LET radiation induces inflammation and persistent changes in markers of hippocampal neurogenesis. *Radiat Res* **164**, 556–560 (2005).
44. DeCarolis, N. A. et al. 56Fe particle exposure results in a long-lasting increase in a cellular index of genomic instability and transiently suppresses adult hippocampal neurogenesis in vivo. *Life Sci Space Res (Amst)* **2**, 70–79. https://doi.org/10.1016/j.lssr.2014.06.004 (2014).
45. Amelchenko, E. M. et al. Cognitive flexibility is selectively impaired by radiation and is associated with differential recruitment of adult-born neurons. *J Neurosci* **43**, 6061–6083. https://doi.org/10.1523/JNEUROSCI.0161-22.2023 (2023).
46. Greene-Schloesser, D. et al. Radiation-induced brain injury: A review. *Front Oncol* **2**, 73. https://doi.org/10.3389/fonc.2012.00073 (2012).
47. Son, Y., Yang, M., Wang, H. & Moon, C. Hippocampal dysfunctions caused by cranial irradiation: a review of the experimental evidence. *Brain Behav Immun* **45**, 287–296. https://doi.org/10.1016/j.bbi.2015.01.007 (2015).
48. Westphal, M., Saladino, A. & Tatagiba, M. Skull base meningiomas. *Adv Exp Med Biol* **1416**, 47–68. https://doi.org/10.1007/978-3-031-29750-2_5 (2023).
49. Goldbrunner, R. et al. EANO guidelines for the diagnosis and treatment of meningiomas. *Lancet Oncol* **17**, e383-391. https://doi.org/10.1016/S1470-2045(16)30321-7 (2016).
50. Ocklenburg, S. & Guo, Z. V. Cross-hemispheric communication: Insights on lateralized brain functions. *Neuron* **112**, 1222–1234. https://doi.org/10.1016/j.neuron.2024.02.010 (2024).
51. Gunturkun, O., Strockens, F. & Ocklenburg, S. Brain lateralization: A comparative perspective. *Physiol Rev* **100**, 1019–1063. https://doi.org/10.1152/physrev.00006.2019 (2020).
52. Zhou, Y. et al. Molecular landscapes of human hippocampal immature neurons across lifespan. *Nature* **607**, 527–533. https://doi.org/10.1038/s41586-022-04912-w (2022).

53. Moreno-Jimenez, E. P., Terreros-Roncal, J., Flor-Garcia, M., Rabano, A. & Llorens-Martin, M. Evidences for adult hippocampal neurogenesis in humans. *J Neurosci* **41**, 2541–2553. https://doi.org/10.1523/JNEUROSCI.0675-20.2020 (2021).
54. Tosoni, G. et al. Mapping human adult hippocampal neurogenesis with single-cell transcriptomics: Reconciling controversy or fueling the debate? *Neuron* **111**, 1714–1731 e1713, https://doi.org/10.1016/j.neuron.2023.03.010 (2023).
55. Nemati, S. S., Sadeghi, L., Dehghan, G. & Sheibani, N. Lateralization of the hippocampus: A review of molecular, functional, and physiological properties in health and disease. *Behav Brain Res* **454**, 114657. https://doi.org/10.1016/j.bbr.2023.114657 (2023).
56. Chen, W. C., Lucas, C. G., Magill, S. T., Rogers, C. L. & Raleigh, D. R. Radiotherapy and radiosurgery for meningiomas. *Neurooncol Adv* **5**, i67–i83. https://doi.org/10.1093/noajnl/vdac088 (2023).
57. Yassa, M. A., Mattfeld, A. T., Stark, S. M. & Stark, C. E. Age-related memory deficits linked to circuit-specific disruptions in the hippocampus. *Proc Natl Acad Sci U S A* **108**, 8873–8878. https://doi.org/10.1073/pnas.1101567108 (2011).
58. Krotkova, O. A., Kaverina, M. Y. & Danilov, G. V. Eye tracking and interhemispheric interaction in the distribution of spatial attention. *Hum. Physiol.* **44**, 175–182. https://doi.org/10.1134/S0362119718020123 (2018).
59. Danilov, G. V. et al. Gaze fixation patterns correlate with visual attention and memory: The results of a pilot study in healthy subjects. *Modern Tech Med* **11**, 54–60. https://doi.org/10.17691/stm2019.11.1.06 (2019).
60. Thiebaut de Schotten, M. et al. A lateralized brain network for visuospatial attention. *Nat Neurosci* **14**, 1245–1246, https://doi.org/10.1038/nn.2905 (2011).
61. Paredes, M. F. et al. Does Adult Neurogenesis Persist in the Human Hippocampus?. *Cell Stem Cell* **23**, 780–781. https://doi.org/10.1016/j.stem.2018.11.006 (2018).
62. Sorrells, S. F. et al. Human hippocampal neurogenesis drops sharply in children to undetectable levels in adults. *Nature* **555**, 377–381. https://doi.org/10.1038/nature25975 (2018).
63. Lucassen, P. J. et al. Limits to human neurogenesis-really?. *Mol Psychiatry* https://doi.org/10.1038/s41380-018-0337-5 (2019).
64. Spalding, K. L. et al. Dynamics of hippocampal neurogenesis in adult humans. *Cell* **153**, 1219–1227. https://doi.org/10.1016/j.cell.2013.05.002 (2013).
65. Elliott, T. et al. Hippocampal neurogenesis in adult primates: a systematic review. *Mol Psychiatry* **30**, 1195–1206. https://doi.org/10.1038/s41380-024-02815-y (2025).
66. Wang, W. et al. Transcriptome dynamics of hippocampal neurogenesis in macaques across the lifespan and aged humans. *Cell Res* **32**, 729–743. https://doi.org/10.1038/s41422-022-00678-y (2022).
67. Simard, S. et al. Spatial transcriptomic analysis of adult hippocampal neurogenesis in the human brain. *J Psychiatry Neurosci* **49**, E319–E333. https://doi.org/10.1503/jpn.240026 (2024).
68. Leskinen, S., Alsalek, S. & Wernicke, A. G. Effects of radiotherapy on the hippocampus and hippocampal neurogenesis: a systematic review of preclinical studies. *Strahlenther Onkol* **201**, 383–397. https://doi.org/10.1007/s00066-024-02341-4 (2025).

Acknowledgements

This work was supported by Russian Science Foundation grant 23-15-00018 to O.K., SBU Healthy Aging Center to G.E., National Institute on Aging grant R01 AG076937 to G.E., and National Institute of Mental Health grant R01 MH134776 to G.E.

Author contributions

Conceptualization: O.A.K., M.V.G., K.V.A., A.A.L., G.E.; design: O.A.K., M.V.G., G.V.D., E.V.E., K.V.A., A.A.L., G.E.; methodology: O.A.K., M.V.G., G.V.D., E.V.E.; investigation: O.A.K., M.V.G., G.V.D., M.Yu.K., A.Yu.K., N.A.F.; radiotherapy: M.V.G., N.A.F.; analysis and interpretation: O.A.K., M.V.G., G.V.D., M.Yu.K., A.Yu.K., E.M.A., K.V.A., A.A.L., G.E.; funding acquisition: O.A.K., G.V.D., G.E.; project administration and coordination: O.A.K., M.V.G., G.V.D., G.E.; writing the manuscript: O.A.K., M.V.G., G.E.; editing the manuscript: O.A.K., M.V.G., G.V.D., E.V.E., E.M.A., K.V.A., A.A.L., G.E. All authors discussed the results and reviewed the manuscript.

Declarations

Competing interests

The authors declare no competing interests.

Additional information

Supplementary Information The online version contains supplementary material available at https://doi.org/10.1038/s41598-025-29852-z.

Correspondence and requests for materials should be addressed to O.A.K. or G.E.